

## **Numerical Estimation Of Mixed Convection Heat Transfer Of Nanofluids Flowing In Horizontal And An Inclined Concentric Annuli**

*Lecture Dr. Khalid Faisal Sultan  
Electromechanical. Eng. Dept  
University of Technology  
E– mail: [ksultan61@yahoo.com](mailto:ksultan61@yahoo.com)*

### **Abstract :**

*A theoretical study has been conducted on a fully developed laminar flow of a nanofluid under the action of mixed convection heat transfer. The nanofluid flows in a horizontal and inclined annuli. The outer cylinder of the annulus is kept adiabatic while the inner cylinder are studied in two cases: Constant Wall Temperature (CWT) and Uniform Heat Flux (UHF). The energy equation was first solved using Alternating Direction Implicit (ADI) method. Then, the momentum and continuity equations were combined to obtain a pressure correction formula. The numerical procedure was implemented on a computer via Fortran power station software. The numerical results for the two boundary conditions considered are given in terms of stream function contours and isotherms for values of Rayleigh number  $Ra$  of  $10^3$ ,  $10^5$  and  $10^6$  and volume fractions  $\Phi$  of 0.5%, 2% and 4%. The effects of nanofluid type and particle size considered in this study. Results showed that the secondary flow created by the natural convection has a significant effect on the heat transfer process.*

*The Nusselt number estimated was higher in the UHF case than that of the CWT case for the same values of Reynolds number ( $Re$ ), Rayleigh number and volume fraction. Nanoparticles concentration did not reveal serious effect on the secondary flow, axial flow profile and the average skin friction coefficient. While increasing volume fraction and Rayleigh number significantly increase Nusselt number.*

**Keywords:** *Nanofluid, Concentric annulus, laminar mixed convection, Heat transfer enhancement*

## التخمين العددي لانتقال الحرارة بالحمل المختلط للموائع النانوية الجارية في الأنابيب الحلقية الأفقية والمائلة

م. د. خالد فيصل سلطان  
قسم الهندسة الكهروميكانيكية  
الجامعة التكنولوجية

### الخلاصة :

دراسة نظرية أجريت على الجريان الطبقي المتكامل النمو للمائع النانوي تحت تأثير انتقال الحرارة بالحمل المختلط. وجريان المائع النانوي يكون من خلال أنابيب حلقية أفقية ومائلة. الأسطوانة الداخلية تدرس في حالتين ثبوت درجة حرارة الجدار و فيض حراري منتظم بينما الأسطوانة الخارجية تكون معزولة لكلا الحالتين. تم حل معادلة الطاقة اولا باستخدام طريقة لاتجاه الضمني المتناوب (ADI) ومن ثم ربط معادلات الزخم بمعادلة الاستمرارية لتكوين معادلة تصحيح الضغط. البرنامج الحاسوبي المستخدم في هذه الدراسة كتب بلغة فورتران الإصدار الرابع والنتائج العددية لكلا الشرطين مثلت بمخططات دالة الجريان ودرجة الحرارة ولقيم عدد رالي ( $Ra=10^3, 10^5, 10^6$ ) ونسب حجوم ( $\Phi = 0.5\%, 2\% \text{ and } 4\%$ ). تأثير نوع المائع النانوي وحجم الجزيئية النانوية وزاوية ميلان الانبوب الحلقي أخذت بالاعتبار في هذه الدراسة أيضا. نتائج الحل العددي أظهرت أن الجريان الثانوي الناتج عن الحمل الحر له تأثير هام على عملية انتقال الحرارة كما إن عدد نسلت مع حالة الفيض الحراري المنتظم (UHF) يكون اكبر من حالة ثبوت درجة الحرارة (CWT) لنفس قيم عدد رينولدز، عدد رالي، ونسب الحجم. تركيز الجزيئات النانوية لا يظهر تأثير هام على الجريان الثانوي، الجريان المحوري الجانبي ومعدل معامل الاحتكاك السطحي بينما زيادة نسب الحجوم وعدد رالي تؤدي إلى زيادة هام في عدد نسلت.

### 1. Introduction

Heat transfer within horizontal and an inclined annuli has many engineering applications such as heat exchangers, solar collectors, thermal storage systems and cooling of electronic components. Several applications use natural convection as the main heat transfer mechanism. Therefore, it is important to understand the thermal behavior of such systems when only natural convection is in effect so that methods to enhance heat transfer characteristics in such systems can be devised. The geometric shape of the cylindrical annulus creates non – uniformity in heat transfer within the annulus. An innovative technique for improving heat transfer is using ultrafine solid particles in a base fluid, which has been used extensively in the past ten years. The term nanofluid refers to fluids in which nano – scale particles are suspended in a base fluid. The enhancement of thermal conductivity of convectional fluids by the suspension of ultra – fine solid particles, has been well known for more than 100 years<sup>[1]</sup>. However, they have not been of interest for practical application due to the problems of sedimentation, erosion, fouling and increased pressure drop in the flow channel. The recent advance in materials technology has made it possible to produce nanometer – size particles that can overcome these problems. The particles are different from

conventional particles (of millimeter or micro – meter size) in that they tend to remain suspended in the fluid and no sedimentation occurs which causes no increase in pressure drop in the flow field <sup>[2]</sup>. Different concepts have been proposed to explain this enhancement in heat transfer. Xuan and Li <sup>[3]</sup> and Xuan and Roetzel <sup>[4]</sup> have identified two causes of improved heat transfer by nanofluids: the increased thermal dispersion due to the chaotic movement of nanoparticles that accelerates energy exchanges in the fluid and the enhanced thermal conductivity of nanofluids. while Keblinski et al.,<sup>[5]</sup> have studied four possible mechanisms that contribute to the increase in nanofluid heat transfer: Brownian motion of the particles, molecular – level layering of the liquid/particle interface, heat transport in the nanoparticles and nanoparticles clustering. The past decade has witnessed extensive work on convective heat transfer using nanofluids. Studies on the enhancement of heat transfer characteristics in forced convection applications were conducted by many researchers. while heat transfer enhancement in natural convection applications has received lesser attention. Khanafer et al. <sup>[6]</sup> studied Copper – Water nanofluids in a two dimensional rectangular enclosure for the case of natural convection. They found that the heat transfer rate increases by increasing the percentage of the suspended particles. Similar enhancement was achieved experimentally by Nnanna et al. <sup>[7]</sup> for Cu nanoparticles in ethylene glycol and by Nnanna and Routhu <sup>[8]</sup> for Alumina–Water nanofluids. Putra et al. <sup>[9]</sup> presented their experimental observations on natural convection of Al<sub>2</sub>O<sub>3</sub> and CuO – water nanofluids inside a horizontal cylinder heated from one end and cooled from the other. Unlike the results of forced convection, they found a systematic and definite deterioration of the natural convective heat transfer, which was dependent on the particle density, concentration, and the aspect ratio of the cylinder. The deterioration increased with particle concentration and was more significant for CuO nanofluids. Wen and Deng<sup>[10]</sup> found that the natural convection heat transfer coefficient in a vessel composed of two discs using TiO<sub>2</sub> nanoparticles decreases by increasing the volume fraction of nanoparticles. Jou and Tzeng <sup>[11]</sup> simulated natural convection heat transfer of Copper – Water nanofluids in a two dimensional enclosure. They reported an increase in heat transfer by the addition of nanoparticles. Recently, Trisaksri and Wongwises, and Wang and Mujumdar <sup>[12]</sup> conducted a literature review on the general heat transfer characteristics of nanofluids. Mirmasoumi and Behzadmehr <sup>[13]</sup> have studied the effects of nanoparticle mean diameter on the heat transfer and flow behavior into a horizontal tube under laminar mixed convection condition. Their calculated results demonstrate that the convection heat transfer coefficient significantly increases with decreasing the nanoparticles means diameter. However, the hydrodynamics parameters were not significantly changed. Annulus appears in many industrial heat exchangers. Therefore, many investigations have been done on the heat transfer mechanisms of an annulus. Among them Srivastava et al. <sup>[14]</sup> experimentally investigated the effect of an unheated length and the annulus ratio on the variations in heat transfer coefficient in the entrance region of an annulus. They showed that the effect of the shape of unheated section becomes significant around  $x/D = 2$ . Gupta and Garg <sup>[15]</sup> numerically studied laminar flow in the hydrodynamic entrance region of an annular tube by

using an implicit finite difference. They found that for a very small annulus ratio the results depart significantly from those for a circular pipe El – Shaarawiy and Alkam <sup>[16]</sup> solved numerically the transient laminar forced convection in the entrance region of an annulus. For different initial thermal conditions, they found that heating the outer boundary produces more pronounced effects than those associated with heating the inner boundary. Recently Lu and Wang <sup>[17]</sup> experimentally studied the convective heat transfer of water flow in a narrow annulus. They showed that the thermal characteristics of fluid flow in an annulus are different from those in circular tubes. Transition from laminar to turbulent occurs at the lower Reynolds number in annuli compared to the one for circular tubes. Nguyen et al. <sup>[18]</sup> experimentally studied heat transfer enhancement of Al<sub>2</sub>O<sub>3</sub>–water nanofluid, flowing inside a closed system, destined for cooling of a microprocessor or an electronic devices. In the turbulent regime with 6.8% particle volume concentration, heat transfer coefficient was found to be increased by as much as 40% compared to that of the base fluid only. The above literature review and the efforts of the previous researchers show the complexity of heat transfer process inside the cylindrical annuli. Despite the numerous researches found in the literature, no work has focused on mixed convection heat transfer inside cylindrical annuli.

The goal of this work is to investigate heat transfer characteristics of mixed convection in the annular horizontal and an inclined concentric cylinders (annuli) using different types of nanofluids. The problem will be investigated numerically by solving the continuity, momentum and energy equations using the finite difference technique. Heat transfer characteristics will be analyzed for various volume fractions of nanoparticles at various Rayleigh numbers.

## 2. Problem Description and Governing Equations

In view of the annular geometry of the problem a cylindrical coordinate system is employed and due to geometrical symmetry, (**Figure.1**) only one half of the annulus is simulated with two cases uniform heat flux and constant wall temperature. The annulus between the two cylinders is filled with water based nanofluid. Three types of nanoparticles are investigated which are Silver, copper and titanium oxide. It is assumed that the base fluid (water) and nanoparticles are in thermal equilibrium and no slip occurs between them. The thermo – physical properties of the base fluid (water) and the three types of nanoparticles forming the nanofluids are given in (**Table 1**). The governing equations for the case of single phase, laminar and steady flow in three dimensional cylindrical coordinates are as follows:

Continuity Equation

$$\frac{\rho_{nf}}{r} (ru)_r + \frac{\rho_{nf}}{r} V_\theta + \rho_{nf} W_z = 0 \quad (1)$$

Momentum Equation

r – Component

$$\rho_{nf} \left( VV_r + \frac{W}{r} V\theta - \frac{W^2}{r} \right) = -P_r + \mu_{nf} \left( V_{rr} + \frac{1}{r} V_r + \frac{1}{r^2} V_{\theta\theta} - \frac{V}{r^2} - \frac{2}{r^2} W_\theta \right) - \rho_{nf} g(\cos\theta \cos\theta)$$

(2)

*q* – Component

$$\rho_{nf} \left( VW_r + \frac{W}{r} W\theta - \frac{VW}{r} \right) = -\frac{1}{r} P_\theta + \mu_{nf} \left( W_{rr} + \frac{1}{r} W_r + \frac{1}{r^2} W_{\theta\theta} - \frac{W}{r^2} + \frac{2}{r^2} W_\theta \right) - \rho_{nf} g(\sin\theta \sin\theta)$$

(3)

Z – Component

$$\rho_{nf} \left( VU_r + \frac{W}{r} U\theta \right) = -P_z + \mu_{nf} \left( U_{rr} + \frac{1}{r} U_r + \frac{1}{r^2} U_{\theta\theta} \right) - \rho_{nf} g(\sin\alpha)$$

(4)

Energy equation

$$\rho_{nf} C_{p,nf} \left( Vt_r + \frac{W}{r} t_\theta + Wt_z \right) = k_{nf} \left[ -\frac{1}{r} \frac{\partial}{\partial r} (rt_r) + \frac{1}{r^2} t_{\theta\theta} + t_{zz} \right]$$

(5)

The properties of nanofluid (fluid containing suspended nanoparticles) are defined as follows:  
Effective thermal conductivity [2]

$$\frac{k_{nf}}{k_f} = \left[ \frac{k_s + (n-1)k_f - (n-1)(k_f - k_s)\Phi}{k_s + (n-1)k_f + (k_f - k_s)\Phi} \right]$$

(6)

Where n is a shape factor and equal to 3 for spherical nanoparticles.

Thermal diffusivity [19].

$$\alpha_{nf} = \frac{k_{nf}}{(1-\Phi)(\rho C_p)_f + \Phi(\rho C_p)_s}$$

(7)

Thermal expansion coefficient [6].

$$\beta_{nf} = \left[ \frac{1}{1 + \frac{(1-\Phi)\rho_f}{\Phi\rho_s}} \frac{\beta_s}{\beta_f} + \frac{1}{1 + \frac{\Phi\rho_s}{(1-\Phi)\rho_f}} \right]$$

(8)

Specific heat [6].

$$Cp_{nf} = \frac{(1-\Phi)(\rho Cp)_f + \Phi(\rho Cp)_s}{(1-\Phi)\rho_f + \Phi\rho_s} \tag{9}$$

Effective viscosity <sup>[19]</sup>.

$$m_{nf} = [123\Phi^2 + 7.3\Phi + 1] \tag{10}$$

**Table .1. Thermo – physical properties of the nanofluids employed.**

Base fluid	Pr	$\rho$ (Kg/m <sup>3</sup> )	Cp (J/kg k)	k (W/m k)	$\beta *10^5$ (k <sup>-1</sup> )	$\alpha *10^5$ (m <sup>2</sup> /s)
Water	6.2	997.1	4179	0.613	21	
<b>Nanoparticles</b>						
Copper (Cu)		8933	385	401	1.67	11.7
Silver (Ag)		10500	235	429	1.89	17.4
Titanium Oxide ( TiO <sub>2</sub> )		4250	686.2	8.9538	0.9	0.31

### 3. Boundary Conditions

**A.** Symmetry lines ( $r_i < r < r_o$  ;  $\Theta = 0$  or  $\pi$ ):

$$W_{\Theta} = 0, W_{r\Theta} \text{ and } T_{\Theta} = 0$$

**B.** 2. Inner cylinder ( $r = r_i$  ;  $0 < \Theta < \pi$ ):

$$W_r = W_{\Theta} = W_z = 0 \text{ and } -k T_r = q$$

**C.** Outer cylinder ( $r = r_o$  ;  $0 < \Theta < \pi$ ):

$$W_r = W_{\Theta} = W_z = 0 \text{ and } T_r = 0$$

**D.** Inlet ( $z = 0$ ) :

$$W_r = W_{\Theta} = 0 , W_z = W_{zi} ; \text{ and } T = T_i$$

### 4. Grid Testing and Code Validation

**Figure.(1)** shows the geometry of the considered problem. Basically, the flow region associated with the polar coordinates (R,Θ) is divided into a grid network which contains the following dimensions ( $\Delta R \times \Delta \theta$ ) for one division as shown in **Figure.(2)**. The number of divisions and nodal points in this case will be (mt×nt) and [(mt+1) × (nt+1)] , respectively, where mt refers to the number of divisions in R direction which changes from (m=1) to

( $m=mt$ ) and equal to  $(1/\Delta R)$ , while ( $nt$ ) refers to the number of divisions in  $\theta$  – direction which changes from ( $n=1$ ) to ( $n=nt$ ) and is equal to  $(\pi/\Delta\theta)$  for one half of the annulus gap because of flow symmetry about the vertical line of the annulus. **Figure.(3)** demonstrates the influence of number of grid points for a test case of fluid confined within the present configuration at  $Ra=10^4$  and  $\Phi =0$ , it is clear that, the grid system of (61\*61) is enough to obtain accurate results. The present code was tested for grid independence by calculating the average Nusselt number around the perimeter of the inner tube as shown in **(Table.2)**. The adopted grid size is (61\*61) nodes. **Figure. (4)** shows the comparison of the present results (secondary flow) with the results of Carlo and Guidice <sup>[20,21]</sup>. The numerical code was tested by comparing the predicted Nusselt numbers with the results of Carlo and Guidice <sup>[21]</sup> who considered the same problem using finite element method. **Figure.(5)** shows that the present results are in excellent agreement  $\pm 3.5$  % with the results of Carlo and Guidice.

$$\text{Relative error} = \frac{Nu_{\text{large grid}} - Nu_{\text{small grid}}}{Nu_{\text{large grid}}} \quad (11)$$

**Table.2. Grid independence tests  $Ra=10^4$**

Grid Size	Water		Nanofluid	
	$Nu_{\text{avg}}$	Relative error	$Nu_{\text{avg}}$	Relative error
15x15	4.7589	—	4.8366	—
20x20	4.6582	- 0.02161	4.7352	-0.02097
25x25	4.4421	- 0.04864	4.5938	-0.04212
35x30	4.4695	$6.130 \times 10^{-3}$	4.6110	$3.7302 \times 10^{-3}$
40x50	4.46902	$-6.7126 \times 10^{-6}$	4.6104	$-1.30145 \times 10^{-4}$
61x61	4.46903	$-2.2376 \times 10^{-6}$	4.6108	$8.6752 \times 10^{-5}$

## 5. Numerical implementation

The governing equations in the cylindrical coordinates (equations 1, 2, 3,4and 5) as well as boundary conditions were discretized by finite difference method. In this study the finite difference equations were derived by using central difference approximation for the partial derivatives except the convective terms for which upwind difference formula was employed. Derivative at the boundary were approximated by three point forward difference. The Alternating Direction Implicit (ADI) method was employed for the solution of energy equation, while the momentum and continuity equations were combined to get the pressure correction formula and solved by the simple algorithm (simple algorithm described in Patankar and Spalding (1972) is used to ensure that continuity of mass is conserved). A time increment  $\Delta t =10^{-5}$  second has been used for  $Ra=10^3,10^5$  and  $10^6$ . In order to accurately understand the influence of nanofluid flowing in the annulus, it is necessary to estimate the

value of local Nusselt number around the inner tube perimeter. Nusselt number will be estimated for various values of Rayleigh number, nanoparticles volume fraction, and annulus inclination angle.

The local Nusselt number at the heated wall (1) is calculated from the temperature gradient at the wall at each time step and takes the following form:

$$Nu_n^k = \frac{T_{R|_{1,n}}^k}{T_1^k} \quad (12)$$

The derivative at the wall  $T_{R|_{1,n}}^k$  is approximated by using three – points forward difference with error order  $O(\Delta R)^2$  and takes the following form

$$T_{R|_{1,n}}^k = \frac{Nu^k}{2\Delta\Delta} [3T_{1,n}^k - 4T_{2,n}^k + T_{3,n}^k] \quad (13)$$

But, the value of  $T_1$  at the location (k) can be calculated from the value of mean Nusselt number around the perimeter of inner cylinder after finishing the step of location (k). As a result, it can be written as follows:

$$T_1^{k+1} = \frac{2\left(\frac{r_2}{r_1} - 1\right)}{Nu^k} \quad (14)$$

and , by substituting Eq.(14) & Eq.(13) into Eq.(12), the Nusselt number around the perimeter of inner cylinder will be as follows:

$$Nu_{nt}^{k+1} = \frac{Nu^k}{4\left(\frac{r_2}{r_1} - 1\right)\Delta R} [3T_{1,n}^k - 4T_{2,n}^k + T_{3,n}^k] \quad (15)$$

The mean Nusselt number around the perimeter of inner cylinder at location (k) is deduced by integrating local Nusselt number as follows:

$$Nu^{k+1} = S Nu^K + (1-S) \frac{2}{\pi} \int_0^\pi Nu_{nt}^{k+1} d\theta \quad (16)$$

The Nusselt number is used to calculate the surface temperature at the location (k+1), but it is found that the boundary conditions cause unstable state in the solution at the value of relaxation factor ( $S = 0$ ). Therefore, the relaxation factor ( $S = 0.8$ ) is used for stability

considerations, <sup>[22]</sup>. The above integral was calculated using Simpson's 1/3 rule method. To show the effect of the nanofluids on heat transfer rate, a variable called Nusselt number ratio (NuR) is introduced with its definition given as:

$$\text{NuR} = \frac{\text{Nuave|with nanofluid}}{\text{Nuave|pure fluid}} \quad (17)$$

If the value of NuR greater is than 1, this indicate that the heat transfer rate is enhanced on that fluid, whereas reduction of heat transfer is indicated when NuR is less than 1.

## 6. Results and discussion

Numerical calculations have been performed for an annulus of radius ratio of 0.5. Three types of nanoparticles are used which are Ag (25nm), Cu (30nm) and TiO<sub>2</sub> (50nm) having volume fractions of (0.5, 2 and 4 %) respectively. **Figures.** (6) and (7) depict secondary flow and temperature for three types of the nanofluids at Rayleigh number ( $Ra=10^5$ ), Reynolds number ( $Re = 200$ ) and  $\alpha = 0$  (horizontal). In general, in horizontal positions, the nanofluid flows up along the inner wall to form vortices having their center in the upper part of the annulus. The vortex strength increases with Rayleigh number, and finally the vortex breaks up into two or more vortices. At small Rayleigh number, the vortex circulation is weak, so it is expected that one cell will be formed in each side about the vertical line of annulus.

The nanofluid rises to top of the annulus and falls slowly toward the centerline annular gap because of buoyancy force. Therefore, a secondary flow patterns appears at the annulus cross section which creates a circular cell. Its position depends on the balance of the buoyancy force and the inertia of the secondary flow at the vertical plane (symmetry plane). The effects of particles concentration on the secondary flow and temperature for two cases CWT and UHF are shown in **Figures.** (6) and (7). Adding Ag (20nm), Cu (30nm) and TiO<sub>2</sub> (50 nm) nanoparticles in pure water increases the effective thermal conductivity of the water and therefore the molecular heat diffusion is augmented. **Figures.** (6) and (7) show that the uniformity of temperature of the nanofluid increases with increasing particle concentration for both CWT and UHFcases. However the center of the secondary flows is located above the horizontal centerline.

The circulation strength is similar approximately between nanofluids and water. It can be noticed in UHF case that a small eddy is formed below the main eddy in the horizontal annuli ( $\alpha = 0$ ). This phenomenon is seen for different values of volume fractions when Re, Ra are kept constants. This small eddy renders the velocity profile unsymmetrical. The isotherms tend to become horizontal, especially in the regions away from and under the inner cylinder, approximating the temperature distribution in a stably stratified nanofluid as shown in **Figures .(6) and (7)**. The secondary flow does not significantly change despite of higher heat flux needed to keep the Rayleigh number constant for higher particles concentration. However, this study did not estimate an optimum nanoparticle volume fraction for heat

transfer. Most likely, there is a point where adding more nanoparticles to the nanofluid becomes counterproductive in removing heat due to agglomeration. It is expected that the heat transfer process in horizontal position is better than other angles of inclinations because of the stronger secondary flow associated with free convection which reduces temperature difference in the annulus. Plot of the contours of the stream and isotherms lines for different inclination angles ( $\alpha = 30^\circ, 60^\circ, 90^\circ$ ), Reynolds number ( $Re = 200$ ) and Rayleigh number ( $Ra = 10^4$ ) can exhibit the form of secondary flow as shown in the figures. (8 & 9).

Plots of isotherms for different inclination angles ranged between horizontal and vertical position are drawn to show the effect of inclination angle on heat transfer. It can be seen from Figures. (8) and (9) that the isotherms form concentric circles around the annulus centerline for the case of vertical annulus ( $\alpha = 90^\circ$ ). These lines be a concentric circles perfectly with the centerline annulus ( $\alpha = 90^\circ$ ) because vanishing effect of free convection on flow field in the tangential & radial direction. In vertical position **Figures.**(8 & 9) reveal the main and secondary flows are in the same direction, so the vortex strength diminishes. The velocities due to buoyancy forces are parallel to the direction of the forced motion; thus, rotational symmetry is retained. This situation leads to one component of the velocity due to buoyancy forces in the same direction of axial velocity because there are no components of buoyancy forces in  $(r, \theta)$  direction compared with the horizontal and inclined positions in which three components of velocity in  $(r, \theta, z)$  directions are formed. Thus, there is no tangential and radial velocities, and the value of stream function in terms of these two velocities is equal to zero.

**Figures.**(8 & 9) shows the isotherms lines contour for  $N=0.5$ ,  $\alpha = 90^\circ$  (vertical), and  $Ra=10^4$ , to CWT and UHF. This is an indication for accuracy of the numerical method used in solution of the governing equations of flow. The figures show on the right hand side the isotherms contour that are nearly circular and have the same center located exactly at the center of annulus. This further indicate little influence of the convective flow on heat transfer. The isotherms in **Figures.**(8) and (9) seem to be closer to each other near the heated inner wall because the natural convection is weak and have a slight effect on the flow field compared with the forced convection. This effect is limited to accelerating the fluid velocity near the heated wall.

The isotherms lines remain in a form of circular lines which have the same center located at the center of annulus and distributed between the temperature of heated inner wall and adiabatic outer wall. **Figure.** (10) shows the shape of the secondary flow for three types of nanofluids considered, namely (Ag (20nm) – pure water), (Cu (30nm) – pure water) and (TiO<sub>2</sub> (50nm) – pure water). The secondary flow tends to be more pronounced in nanofluids than in the pure water for both CWT and UHF cases. However the temperature profile does not seriously changes. Adding nanoparticles to pure water increases the effective thermal conductivity and molecular heat diffusion. This make the temperature profile more uniform. The axial velocity profile also does not change seriously for the three nanofluids studied. **Figure.** (11) Shows the axial profile of the peripheral Nusselt number with different

inclination angles ( $\alpha=0^0, 30^0, 45^0, 60^0, 90^0$ ), Rayleigh number ( $Ra=10^5$ ), Reynolds number ( $Re = 400$ ) and volume fraction ( $\Phi= 4 \%$ ).

The left and right sides of these Fig. show the value of Nusselt number in horizontal annulus is greater than that of vertical annulus. This is due to the formation of secondary flow and the convection currents & eddies associated with natural convection in horizontal annulus. Therefore , Nusselt number decrease with increasing the inclination angle above the horizontal level. As it is clearly seen increasing the Rayleigh number augments the buoyancy force and enhances Nusselt number at the fully developed region. The nanoparticle Ag (20 nm) is smaller than both nanoparticles Cu (30nm) and  $TiO_2$  (50nm) so heat transfer for the nanofluid (Ag (20nm) – pure water) is higher than both nanofluids (Cu ( 30 nm) – pure water) and ( $TiO_2$ ( 50 nm) – pure water) due to small particles size of silver, this makes the random motion larger and the convection effect become more pronounced.

The three types of nanofluids, with 20 nm, 30 nm and 50 nm particles showed higher heat transfer rate than the base fluid.

The metallic nanoparticles give higher heat transfer enhancement than nonmetallic nanoparticles (oxides) due to the higher thermal conductivity of the metallic nanoparticles. **Figure (12)** shows the average skin friction coefficient around tube periphery in the CWT case (on the left side) and the UHF case (on the right side) for nanofluid (Ag (20nm) – pure water) at constant Rayleigh number ( $Ra=10^5$ ), Reynolds number ( $Re = 400$ ), volume fraction ( $\Phi=0, 0.5, 4 \%$ ) and different inclination angles of the annulus ( $\alpha=0^0, 30^0, 45^0, 60^0, 90^0$ ). In spite of augmenting the Nusselt number by increasing the nanoparticles concentration, the skin friction does not change.

As it was seen in the previous figures, the velocity profiles and the secondary flow are not significantly affected by the nanoparticles concentration. Also at high Rayleigh numbers increasing the nanoparticles volume fractions does not have significant effect on skin friction coefficient. In general, increasing the annulus inclinations augments the flow acceleration near wall and consequently higher skin friction occurs.

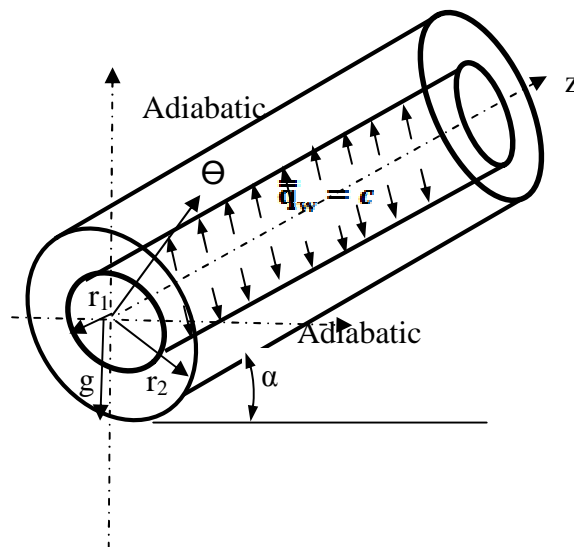


**Fig. (1) Physical representation of the problem in polar coordinate**



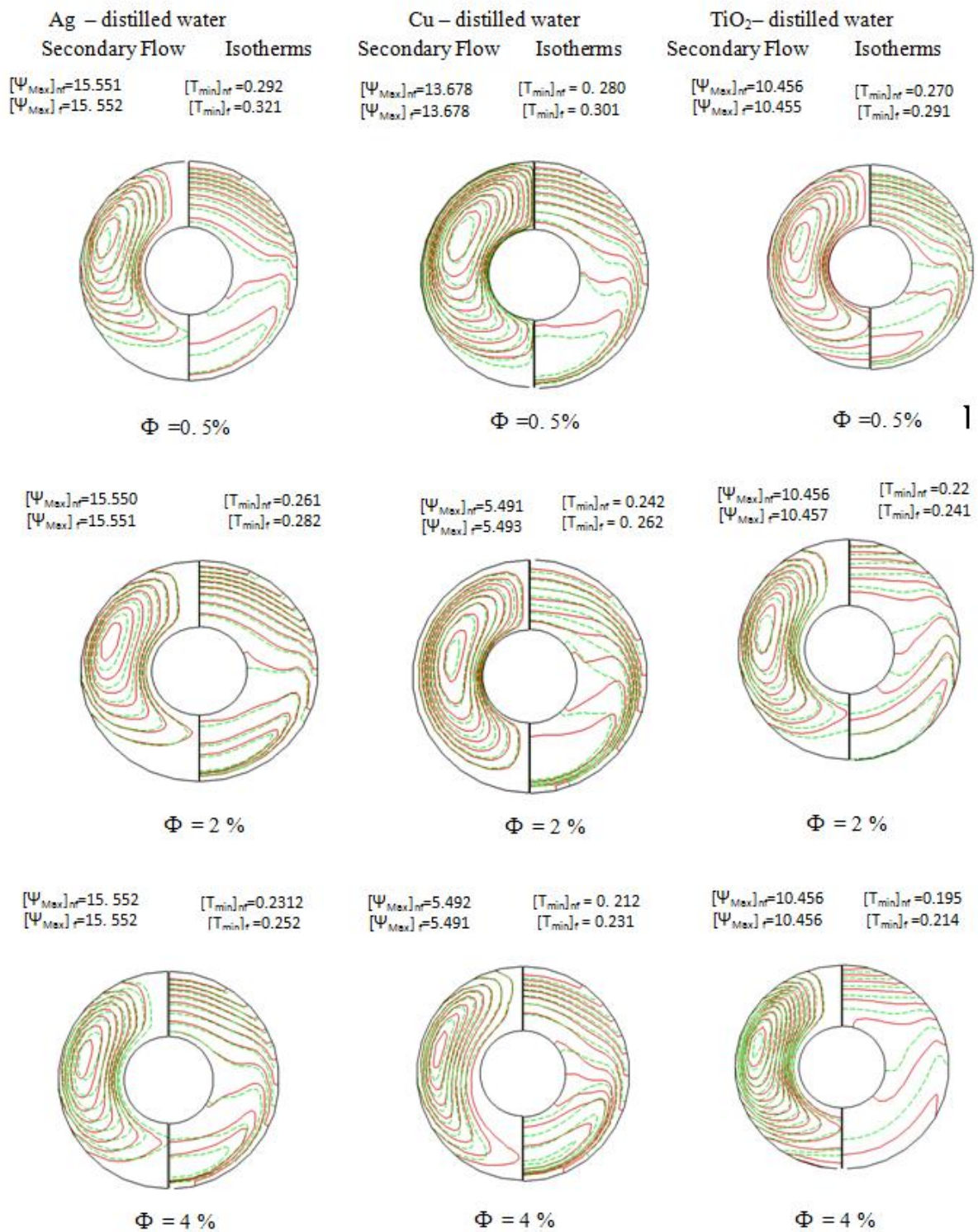


**Fig.(6) : Secondary flow (on the left) and Isotherms (on the right) for Ag, Cu , TiO<sub>2</sub> – pure water nanofluids ( — ) and water ( - - - ) with different  $\Phi$ ,  $Re=200$  ,  $Ra=10^5, \alpha = 0^0$  and CWT**

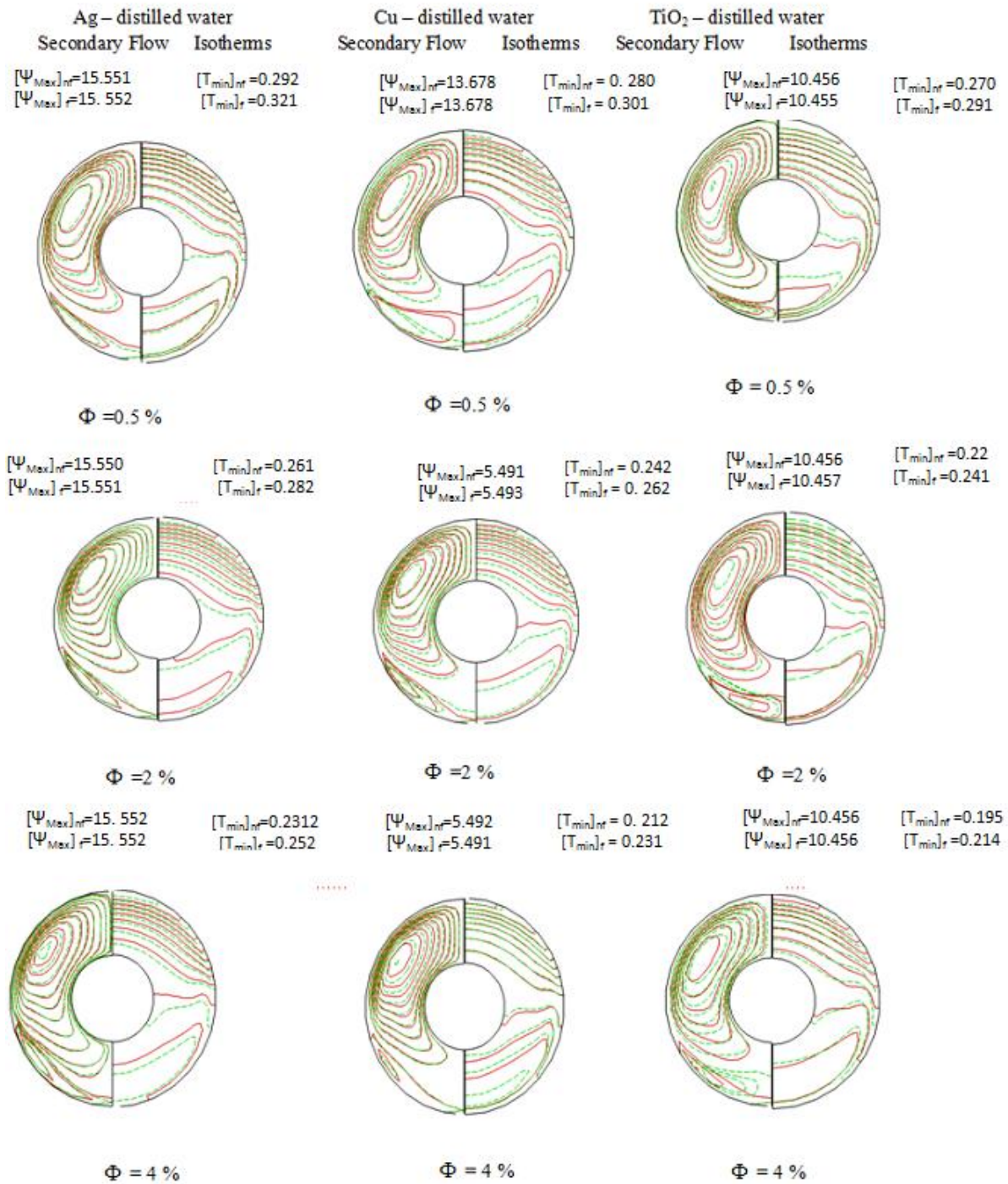
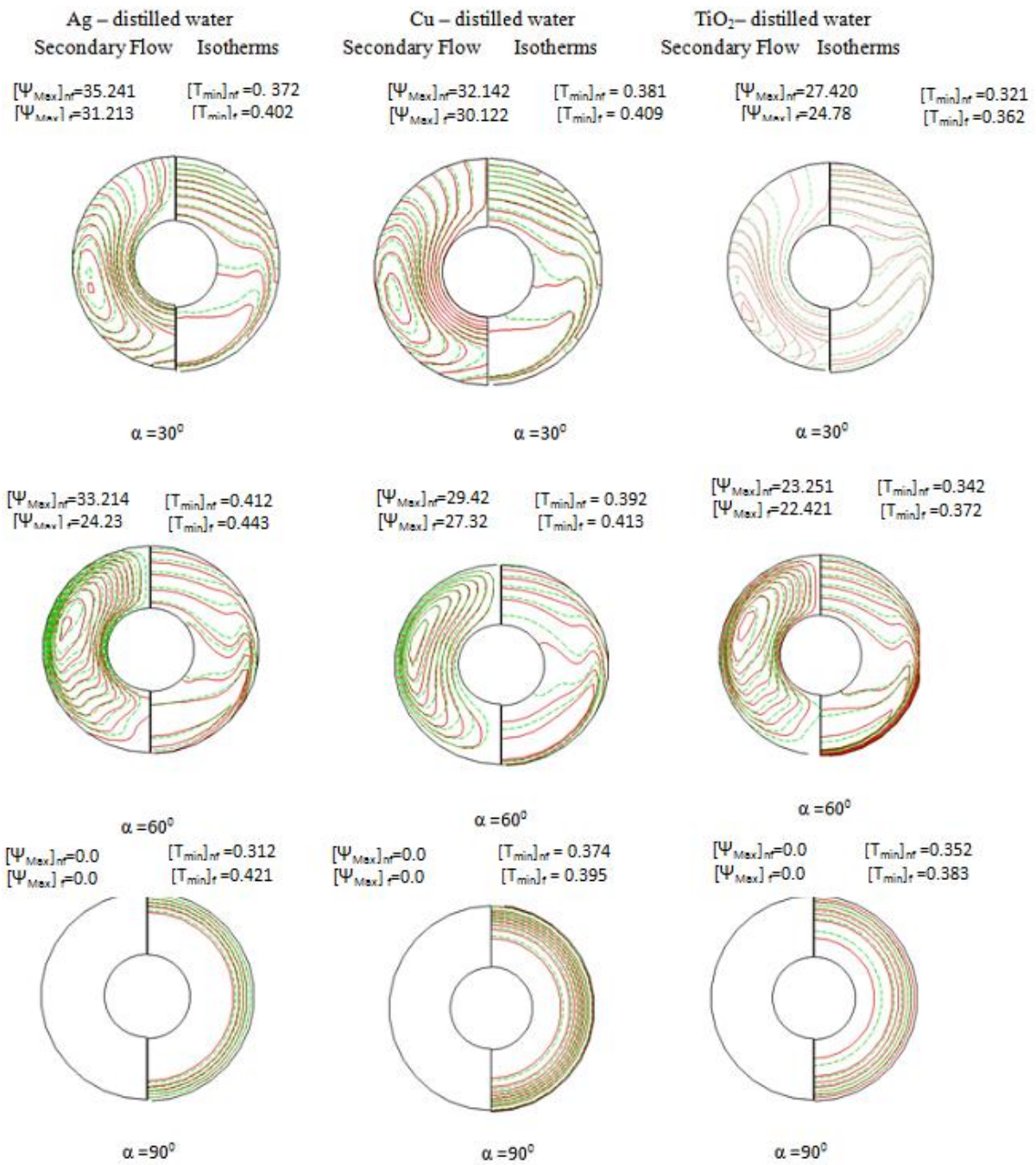
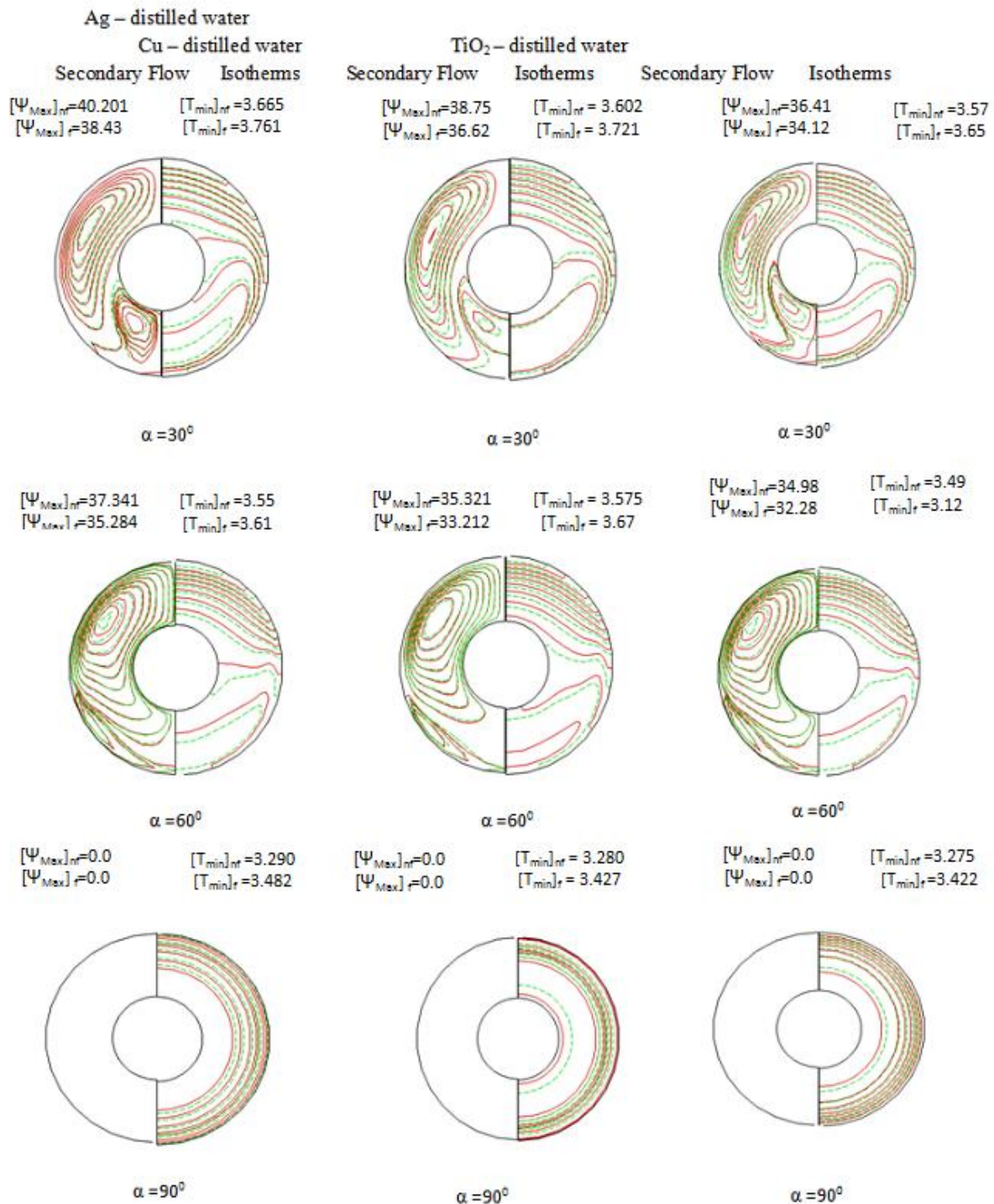


Fig. (7) : Secondary flow (on the left) and Isotherms (on the right) for Ag, Cu , Ti O<sub>2</sub> – distilled water nanofluids ( — ) and water ( - - - ) with different  $\Phi$  , Re=200 , Ra=10<sup>5</sup> and  $\alpha =0^0$  and UHF



**Fig. (8) : Secondary flow (on the left) and Isotherms (on the right) for Ag, Cu ,TiO<sub>2</sub> – distilled water nanofluids ( — ) and water ( - - - ) with different angle , Re=200, Ra=10<sup>4</sup> ,  $\Phi = 4\%$  and CWT**



**Fig. (9) : Secondary flow (on the left) and Isotherms (on the right) for Ag, Cu ,TiO<sub>2</sub> – distilled water nanofluids ( — ) and water ( - - - ) with different angle , Re=200, Ra=10<sup>4</sup>,  $\Phi$  = 4% and UHF**

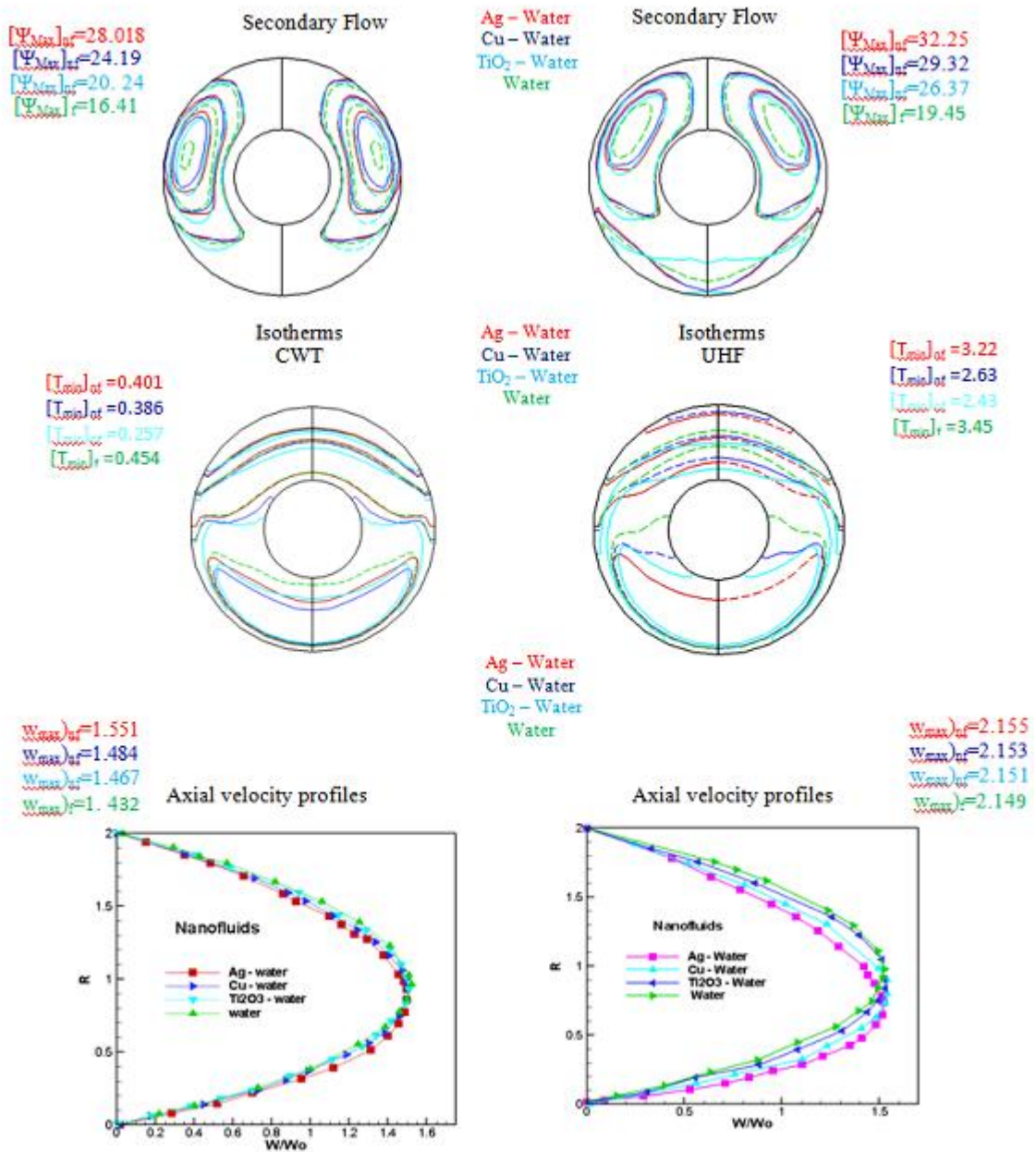


**Fig. (10) : Groups secondary flow, isotherms, adiabatic and axial velocity for fully developed laminar flow in annulus tube for CWT case (on the left) and UHF case (on the right) to Ag, Cu and TiO<sub>2</sub> – water nanofluids and water (----) with different Ra , Φ and Re=400**

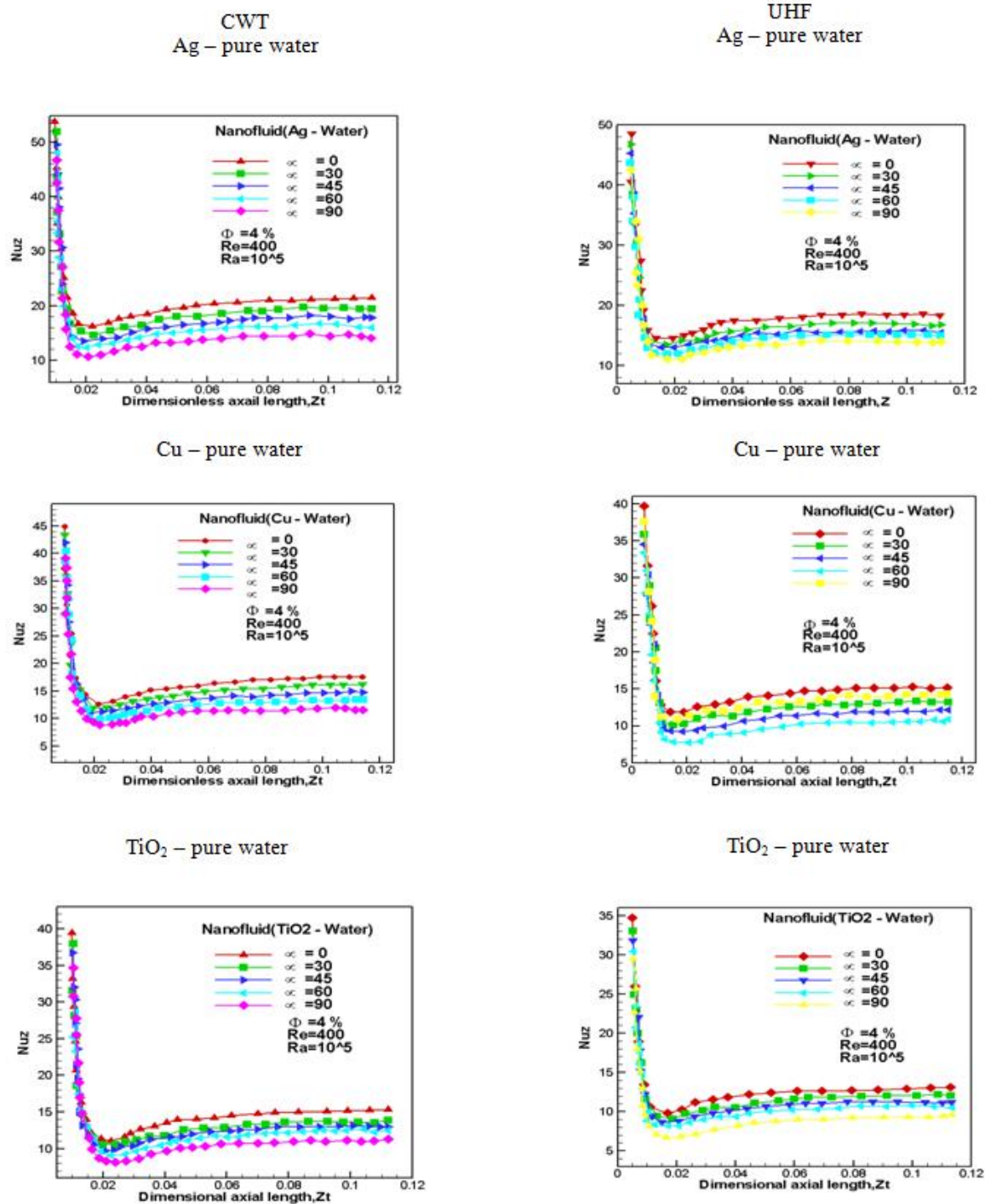


Fig. (11): Axial profile of the peripheral average Nusselt number to CWT and UHF for Cu, Ag and TiO<sub>2</sub> – pure water nanofluids with different angles, Ra=10<sup>5</sup> and Re=400, Φ=4%

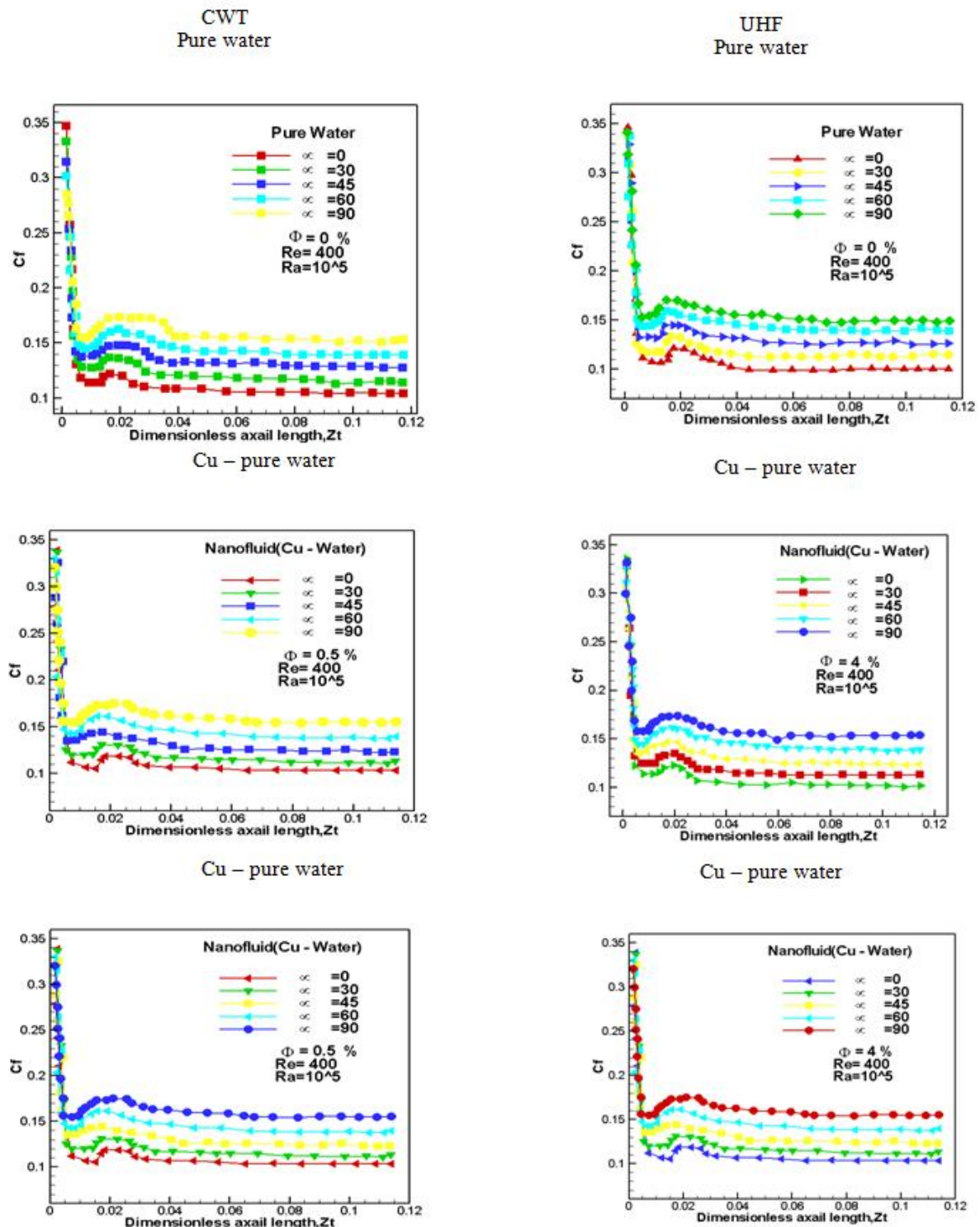


Fig. (12) : Axial profile of the peripheral average skin friction coefficient to CWT and UHF for nanofluid (Cu – pure water) with different  $\Phi$  , $Ra=10^5$ and  $Re=400$

## 7. Conclusion

The following conclusions can be drawn from the present study:

1. velocity fluid and heat transfer rate are increasing generally in nanofluid case compared with pure fluid case.
2. The type of nanofluid is a key factor for heat transfer enhancement. The highest values to lowest of Nu are obtained for Ag (20 nm), Cu (30 nm) and TiO<sub>2</sub> (50 nm) nanoparticles respectively.
3. Nusselt number ratio increases with Rayleigh number at constant volume fraction and increases with volume fraction at constant Rayleigh number.
4. The nanoparticles concentration does not have significant effect on the secondary flow, axial velocity profile and the average skin friction coefficient around annulus periphery.
5. Skin friction coefficient is augmented by increasing the annulus inclinations.
6. The heat transfer enhancement with uniform heat flux is higher than that of constant wall temperature when nanofluids are used.
7. The metallic nanoparticles give higher heat transfer enhancement than nonmetallic nanoparticles (oxides) due to the higher thermal conductivity of metallic nanoparticles.

## 8. Reference

1. S. Lee, S.U.S. Choi, J.A. Eastman, Measuring thermal conductivity of fluids containing oxide nanoparticles, *Journal of Heat Transfer* 121,(1999),280–289.
2. W. Daungthongsuk, S. Wongwises, A critical review of convective heat transfer nanofluids, *Renewable and Sustainable Energy Reviews* 11, (2007),797–817.
3. Xuan, Y.M., Li, Q., Heat transfer enhancement of nanofluids. *Int. J. Heat Fluid Flow* 21, (2000) 58–64.
4. Xuan, Y.M., Roetzel, W., Conceptions for heat transfer correlation of nanofluids. *Int. J. Heat Mass Transf.* 43 (19), (2000),3701–3707.
5. Koblinski, P., Phillpot, S.R., Choi, S.U.S., Eastman, J.A., Mechanisms of heat flow in suspensions of nano-sized particles (nanofluid). *Int. J. Heat Mass Transf.* 45, (2002) 855–863.
6. K. Khanafer, K. Vafai, M. Lightstone, Buoyancy – driven heat transfer enhancement in a two – dimensional enclosure utilizing nanofluids, *International Journal of Heat and Mass Transfer* 46, (2003) ,3639 – 3653.
7. A.G.A. Nanna, T. Fistrovich, K. Malinski, S.U.S. Choi, Thermal transport phenomena in buoyancy-driven nanofluids, *Proc. ASME Int. Mech. Eng. Congress RD&D Expo.,IMECE2004-62059, Anaheim, CA, (2004), pp. 1–8.*

8. A.G.A. Nnanna, M. Routhu, Transport phenomena in buoyancy driven nanofluids – Part II, Proc. ASME Summer Heat Transfer Conf., SHTC – 72782, San Francisco, CA, (2005), pp. 1–8.
9. N. Putra, W. Roetzel, S.K. Das, Natural convection of nanofluids, Heat and Mass Transfer 39, (8–9), (2003) 775–784.
10. D. Wen, Y. Deng, Formulation of nanofluids for natural convective heat transfer applications, International Journal of Heat and Fluid Flow 26 ,(6) ,(2005), 855 – 864.
11. R.-Y. Jou, S.-C. Tzeng, Numerical research of nature convective heat transfer enhancement filled with nanofluids in a rectangular enclosure, International Communications in Heat and Mass Transfer 33 ,(2006), 727–736.
12. X.-Q. Wang, A.S. Mujumdar, Heat transfer characteristics of nanofluids: a review, International Journal of Thermal Sciences 46 ,(2007), 1–19.
13. S. Mirmasoumi, A. Behzadmehr, Effect of nanoparticles mean diameter on mixed convection heat transfer of a nanofluid in a horizontal tube, Int. J. Heat Fluid Flow 29, (2008), 557–566.
14. N.C. Srivastava, F. Bakhtar, F.K. Bannister, An investigation into thermal boundary layer growth in the entrance region of an annulus, Int. J. Heat Mass Transf. 14 ,(1973), 49–59.
15. S.C. Gupta, V.K. Garg, Developing flow in a concentric annulus, Comput. Meth. Appl. Mech. 28,(1981), 27–35.
16. M.A.I. El-Shaarawi, M.K. Alkam, Transient forced convection in the entrance region of concentric annuli, Int. J. Heat Mass Transf. 35 ,(1992), 3335–3344.
17. G. Lu, J. Wang, Experimental investigation on heat transfer characteristics of water flow in a narrow annulus, Appl. Therm. Eng. 28 ,(2008),8–13.
18. C.T. Nguyen, G. Roy, C. Gauthier, N. Galanis, Heat transfer enhancement using  $\text{Al}_2\text{O}_3$  –water nanofluid for an electronic liquid cooling system, Appl. Therm. Eng. 27 (2007) 1501–1506.
19. Barozzi, Sabbagh ,G.S., Zan chini, et al, "Experimental investigation of combined forced and free convection in Horizontal and inclined tubes". Meccanica 20, (1985),18–27.
20. Maiga, S.E., Nguyen, C.T., Galanis, N., Roy, G., "Heat transfer behaviors of Nano fluids in a uniformly heated tube". Super Lattices Micro structure. 35 (3 – 6), (2004), 543–557.
21. Carlo. N, Guidice .S.D, " Finite element analysis of laminar mixed convection in the entrance region of horizontal annuli duct "Numer, Heat Transfer , Part A,29, (1996),PP 313 – 330.
22. D. H. Anderson, J. C. Tannehill, and R. H. Plecher“ Computational Fluid Mechanics and Heat Transfer” Hemisphere. Washington, DC (1984)

## 9. Nomenclature

$r_1$	Inner radius of inner cylinder	m
$r_2$	Outer radius of inner cylinder	m
$Cp_{nf}$	Specific heat of nanofluid at constant pressure	kJ/kg. °C
g	Gravity acceleration	m/s <sup>2</sup>
G	Dimensionless gravity acceleration	–
h	Heat transfer coefficient	W/m <sup>2</sup> . °C
p	Pressure	N/m <sup>2</sup>
$R, \Theta, Z$	Dimensionless cylindrical coordinates	–
Nu	Nusselt number	–
S	Relaxation factor	–
T	Temperature	°C
u	Radial velocity component ( r )	m/s
v	Tangential velocity component ( $\Theta$ )	m/s
w	Axial velocity component ( z )	m/s
$k_{nf}$	Thermal conductivity of the nanofluid	W/m. °C
P	Dimensionless pressures	–
$d_p$	Particle diameter	nm
UHF	Uniform heat flux	–
CWT	Constant wall temperature	–
ADI	Alternating direction implicit	–

### Creak Symbols

$\alpha$	Angle of inclination of tube	degree
$a_{nf}$	Thermal diffusivity of the nanofluid	m <sup>2</sup> /s
$b_{nf}$	Thermal Expansion Coefficient of the nanofluid	1/°C
$\mu_{nf}$	Dynamic viscosity of the nanofluid	kg/m.s
$\nu_{nf}$	Kinematic viscosity of the nanofluid	m <sup>2</sup> /s
$\rho_{nf}$	Density of the nanofluid	kg/m <sup>3</sup>
$\Omega$	Vorticity	1/s
$\Psi$	Stream function	m <sup>2</sup> /s
$\Phi$	Volume fraction	

### Subscripts

m	Mean
mt	Number of radial points in the numerical mesh network

nt	Number of tangential points in the numerical mesh network	
s	Solid	
w	Wall	
r		$\frac{\partial}{\partial r}$
rr		$\frac{\partial^2}{\partial r^2}$
rrr		$\frac{\partial^3}{\partial r^3}$
e		$\frac{\partial}{\partial q}$
ee		$\frac{\partial^2}{\partial q^2}$
eee		$\frac{\partial^3}{\partial q^3}$